ON REPRESENTATIONS OF THE HELMHOLTZ GREEN'S FUNCTION

GREGORY BEYLKIN

ABSTRACT. We consider the free space Helmholtz Green's function and split it into the sum of oscillatory and non-oscillatory (singular) components. The goal is to separate the impact of the singularity of the real part at the origin from the oscillatory behavior controlled by the wave number k. The oscillatory component can be chosen to have any finite number of continuous derivatives at the origin and can be applied to a function in the Fourier space in $\mathscr{O}\left(k^d \log k\right)$ operations. The non-oscillatory component has a multiresolution representation via a linear combination of Gaussians and is applied efficiently in space.

Since the Helmholtz Green's function can be viewed as a point source, this partitioning can be interpreted as a splitting into propagating and evanescent components. We show that the non-oscillatory component is significant only in the vicinity of the source at distances $\mathscr{O}\left(c_1 k^{-1} + c_2 k^{-1} \log_{10} k\right)$, for some constants c_1, c_2, whereas the propagating component can be observed at large distances.

1. INTRODUCTION

In this paper we consider the free space Helmholtz Green's function given by

$$G(r) = \begin{cases} \dfrac{1}{4\pi}\dfrac{e^{ikr}}{r} = \dfrac{1}{4\pi}\dfrac{\cos(kr)}{r} + \dfrac{i}{4\pi}\dfrac{\sin(kr)}{r} & \text{in dimension } d=3, \\[2ex] \dfrac{i}{4}H_0^{(1)}(kr) = -\dfrac{1}{4}Y_0(kr) + \dfrac{i}{4}J_0(kr) & \text{in dimension } d=2, \end{cases} \tag{1.1}$$

where $H_0^{(1)}$ is the Hankel function of the first kind, J_0 and Y_0 are the Bessel functions of the first and second kind, $r = \|\mathbf{x}\| = \left(\sum_{j=1}^d x_j^2\right)^{1/2}$ denotes the Euclidean norm of the vector $\mathbf{x}$ and $k > 0$. We separate G into the sum of oscillatory and non-oscillatory (singular) components. The oscillatory component can be chosen to have any finite number of continuous derivatives at $r = 0$. As far as we know, previous approaches to split G in this manner did not allow to choose the number of smooth derivatives at $r = 0$. As in [7, 6], the oscillatory component can be applied to a function in the Fourier space in $\mathscr{O}\left(k^d \log k\right)$ operations. The non-oscillatory component has a multiresolution representation via a linear combination of Gaussians and is applied efficiently in space.

Our approach is a modification of that in [7, 6] leading to explicit formulas. The goal is to separate the impact of the singularity of the real part of (1.1) at the origin from the oscillatory behavior controlled by the wave number k. Specifically, we want the number of derivatives at the origin of the oscillatory component to be user selected and the non-oscillatory component to have a multiresolution representation via a linear combination of Gaussians. For non-oscillatory kernels integral representations involving Gaussians lead to efficient multiresolution approximations (see e.g. [18, 8, 4, 9, 10, 5, 17, 1]), i.e. when approaching a singularity the domain of integration automatically shrinks leading to fast algorithms for application of such kernels. We want a similar representation of the non-oscillatory component of the Helmholtz Green's function (1.1).

Since G in (1.1) can be interpreted as a point source, a physical interpretation of splitting it into oscillatory and non-oscillatory components may be viewed as a splitting into propagating and evanescent components.

Key words and phrases. Free space Helmholtz Green's function, oscillatory and non-oscillatory components, representation via a linear combination of Gaussians.

Indeed, we show that the non-oscillatory component is significant only in the vicinity of the source at distances $\mathscr{O}\left(c_1 k^{-1} + c_2 k^{-1}\log_{10} k\right)$, for constants c_1, c_2, whereas the propagating component can be observed at large distances.

2. Preliminaries

2.1. **Green's functions.** The free space Green's function (1.1) of the Helmholtz equation satisfies

$$\Delta G(\mathbf{x}) + k^2 G(\mathbf{x}) = -\delta(\mathbf{x}), \tag{2.1}$$

and, on taking the Fourier transform of (2.1), we obtain

$$\widehat{G}(\|\mathbf{p}\|) = \frac{1}{\|\mathbf{p}\|^2 - k^2}, \tag{2.2}$$

where $\mathbf{p} \in \mathbb{R}^d$, $d = 2,3$, We use the Fourier transform defined as

$$\widehat{f}(\mathbf{p}) = \int_{\mathbb{R}^d} f(\mathbf{x})\, e^{-i\mathbf{x}\cdot\mathbf{p}} d\mathbf{x} \tag{2.3}$$

and its inverse as

$$f(\mathbf{x}) = \frac{1}{(2\pi)^d} \int_{\mathbb{R}^d} \widehat{f}(\mathbf{p})\, e^{i\mathbf{x}\cdot\mathbf{p}} d\mathbf{p}. \tag{2.4}$$

The inverse Fourier transform of $\widehat{G}$ is a singular integral and we use regularization (see [7])

$$G(\mathbf{x}) = \lim_{\lambda\to 0^+} \frac{1}{(2\pi)^d} \int_{\mathbb{R}^d} \frac{e^{i\mathbf{x}\cdot\mathbf{p}}}{\|\mathbf{p}\|^2 - (k+i\lambda)^2} d\mathbf{p}, \tag{2.5}$$

which yields the outgoing Green's functions (1.1) satisfying the Sommerfeld radiation condition

$$\lim_{r\to\infty} r^{\frac{d-1}{2}} \left(\frac{\partial G}{\partial r} - ikG\right) = 0. \tag{2.6}$$

Following [7], we define

$$\hat{G}_\lambda(p) = \frac{1}{p^2 - (k+i\lambda)^2} = \frac{1}{2p}\left(\frac{1}{p-k-i\lambda} + \frac{1}{p+k+i\lambda}\right)$$

and separate its real and imaginary parts

$$\mathscr{R}e\left(\hat{G}_\lambda(p)\right) = \frac{1}{2p}\left(\frac{p-k}{(p-k)^2+\lambda^2} + \frac{p+k}{(p+k)^2+\lambda^2}\right) \tag{2.7}$$

and

$$\mathscr{I}m\left(\hat{G}_\lambda(p)\right) = \frac{1}{2p}\left(\frac{\lambda}{(p-k)^2+\lambda^2} - \frac{\lambda}{(p+k)^2+\lambda^2}\right). \tag{2.8}$$

We observe that the limit

$$\lim_{\lambda\to 0^+} \mathscr{I}m\left(\hat{G}_\lambda(p)\right) = \frac{\pi}{2p}\left(\delta(p-k) - \delta(p+k)\right) \tag{2.9}$$

is a generalized function (see e.g. [12, Chapter III, section 1.3]) corresponding to integration over the sphere in the Fourier domain. Using e.g. [14, Section 4.1], we have

$$\lim_{\lambda\to 0^+} \int_0^\infty \frac{1}{2p}\left(\frac{p-k}{(p-k)^2+\lambda^2} + \frac{p+k}{(p+k)^2+\lambda^2}\right) d\rho = \text{p.v.}\int_0^\infty \frac{1}{p^2-k^2} d\rho,$$

so that

$$\mathscr{R}e\left(G(\mathbf{x})\right) = \frac{1}{(2\pi)^d}\,\text{p.v.}\int_{\mathbb{R}^d} \frac{e^{i\mathbf{x}\cdot\mathbf{p}}}{\|\mathbf{p}\|^2 - k^2} d\mathbf{p}, \tag{2.10}$$

where the principal value is considered about $\|\mathbf{p}\| = k$.

3. Splitting of the Green's function in the Fourier domain

We start with

Lemma 1. *For $n \geq 1$ and $p \neq k$ we have*

$$\frac{1}{p^2-k^2} - \widehat{g}_n(p,k) = \frac{1}{p^2-k^2}\frac{\left(2k^2\right)^n}{\left(p^2+k^2\right)^n} = \mathscr{O}\left(\frac{1}{p^{2n+2}}\right), \tag{3.1}$$

where

$$\widehat{g}_n(p,k) = \sum_{j=0}^{n-1} \frac{\left(2k^2\right)^j}{\left(p^2+k^2\right)^{j+1}}. \tag{3.2}$$

Proof. We have

$$\begin{aligned}
\widehat{g}_n(p,k) &= \frac{1}{p^2+k^2}\sum_{j=0}^{n-1}\frac{\left(2k^2\right)^j}{\left(p^2+k^2\right)^j} \\
&= \frac{1}{p^2+k^2}\left(1-\frac{\left(2k^2\right)^n}{\left(p^2+k^2\right)^n}\right)\left(1-\frac{2k^2}{p^2+k^2}\right)^{-1} \\
&= \frac{1}{p^2-k^2}\left(1-\frac{\left(2k^2\right)^n}{\left(p^2+k^2\right)^n}\right) \\
&= \frac{1}{p^2-k^2} - \frac{1}{p^2-k^2}\frac{\left(2k^2\right)^n}{\left(p^2+k^2\right)^n}
\end{aligned}$$

and arrive at (3.1) as an algebraic identity for $p \neq k$. □

Using Lemma 1, we obtain the splitting of (2.2) in the Fourier domain as

$$\widehat{G}(\|\mathbf{p}\|) = \widehat{g}_n(\|\mathbf{p}\|,k) + \widehat{g}_{n,oscill}(\|\mathbf{p}\|,k), \tag{3.3}$$

where

$$\widehat{g}_{n,oscill}(\|\mathbf{p}\|,k) = \frac{1}{\|\mathbf{p}\|^2-k^2}\frac{\left(2k^2\right)^n}{\left(\|\mathbf{p}\|^2+k^2\right)^n} \tag{3.4}$$

and

$$\widehat{g}_n(\|\mathbf{p}\|,k) = \sum_{j=0}^{n-1}\frac{\left(2k^2\right)^j}{\left(\|\mathbf{p}\|^2+k^2\right)^{j+1}}. \tag{3.5}$$

The rate of decay of $\widehat{g}_{n,oscill}$ in the Fourier domain for $\|\mathbf{p}\| > k$ is $\mathscr{O}\left(\|\mathbf{p}\|^{-2n-2}\right)$ so that the volume of its significant support is proportional to k^d. Following [7, 6], we have

$$\widehat{G}(\|\mathbf{p}\|) = \frac{1}{2\|\mathbf{p}\|}\left(\frac{1}{\|\mathbf{p}\|-k}+\frac{1}{\|\mathbf{p}\|+k}\right) =$$
$$\frac{1}{2\|\mathbf{p}\|}\int_0^\infty\left[\left(\|\mathbf{p}\|-k\right)e^{-s(\|\mathbf{p}\|-k)^2}+\left(\|\mathbf{p}\|+k\right)e^{-s(\|\mathbf{p}\|+k)^2}\right]ds$$

yielding

$$\widehat{g}_{n,oscill}(\|\mathbf{p}\|,k) = \frac{2^{n-1}k^{2n}}{\left(\|\mathbf{p}\|^2+k^2\right)^n}\frac{1}{\|\mathbf{p}\|}\int_0^\infty\left[\left(\|\mathbf{p}\|-k\right)e^{-s(\|\mathbf{p}\|-k)^2}+\left(\|\mathbf{p}\|+k\right)e^{-s(\|\mathbf{p}\|+k)^2}\right]ds,$$

or

$$\widehat{g}_{n,oscill}\left(\left\|\mathbf{p}\right\|,k\right)=\frac{2^{n-1}k^{2n}}{\left(\left\|\mathbf{p}\right\|^{2}+k^{2}\right)^{n}}\frac{1}{\left\|\mathbf{p}\right\|}\int_{-\infty}^{\infty}\left[\left(\left\|\mathbf{p}\right\|-k\right)e^{-e^{t}\left(\left\|\mathbf{p}\right\|-k\right)^{2}}+\left(\left\|\mathbf{p}\right\|+k\right)e^{-e^{t}\left(\left\|\mathbf{p}\right\|+k\right)^{2}}\right]e^{t}dt, \tag{3.6}$$

where $\mathbf{p}\in\mathbb{R}^{d}$, $d=2,3$. The integral in (3.6) is a multiresolution representation of $\widehat{g}_{n,oscill}$ centered at the singularity $\left\|\mathbf{p}\right\|=k$. This representation allows us to implement the principal value limit (see e.g. (2.10)) by simply ignoring fine scales since, at some point, their contribution is negligible. Effectively it amounts to replacing the upper limit in the integral in (3.6) by a carefully chosen finite value. Discretizing (3.6) leads to an approximation of $\widehat{g}_{n,oscill}$ via a linear combination of smooth (rotationally invariant) kernels similar to that obtained in [7]. We refer to [7] for the details of applying $\widehat{g}_{n,oscill}$ to a function via an algorithm of complexity $\mathcal{O}\left(k^{d}\log k\right)$.

4. Spatial representations in $\mathbb{R}^{3}$

While the oscillatory component is applied efficiently in the Fourier domain due to its rapid decay, the non-oscillatory component decays slowly in the Fourier domain but its application is efficient in space. We start by computing spatial representations in $\mathbb{R}^{3}$ since these are different in dimensions $d=3$ and $d=2$.

Lemma 2. *The inverse Fourier transform of the non-oscillatory component (3.5) is given by*

$$g_{n}\left(r,k\right)=\frac{1}{4\pi}\frac{e^{-kr}}{r}\left(1+\sum_{j=1}^{n-1}\frac{1}{2^{j-1}j!}\sum_{m=0}^{j-1}\frac{(2j-m-2)!2^{m}}{m!\left(j-m-1\right)!}\left(kr\right)^{m+1}\right) \tag{4.1}$$

Computing g_n for $n=1,2,\dots$ we obtain

$$\begin{aligned}
g_{1}\left(r,k\right) &= \frac{1}{4\pi}\frac{e^{-kr}}{r}\\
g_{2}\left(r,k\right) &= \frac{1}{4\pi}\frac{e^{-kr}}{r}\left(1+kr\right)\\
g_{3}\left(r,k\right) &= \frac{1}{4\pi}\frac{e^{-kr}}{r}\left(1+\frac{3}{2}kr+\frac{1}{2}\left(kr\right)^{2}\right)\\
g_{4}\left(r,k\right) &= \frac{1}{4\pi}\frac{e^{-kr}}{r}\left(1+2kr+\left(kr\right)^{2}+\frac{1}{6}\left(kr\right)^{3}\right)\\
g_{5}\left(r,k\right) &= \frac{1}{4\pi}\frac{e^{-kr}}{r}\left(1+\frac{21}{8}kr+\frac{13}{8}\left(kr\right)^{2}+\frac{5}{12}\left(kr\right)^{3}+\frac{1}{24}\left(kr\right)^{4}\right)\\
&\cdots,
\end{aligned} \tag{4.2}$$

where $r=\left\|\mathbf{x}\right\|$.

Proof. Computing the inverse Fourier transform of rotationally invariant function (3.5) in dimension $d=3$, we have

$$g_{n}\left(r,k\right)=\frac{1}{\left(2\pi\right)^{3}}\int_{\mathbb{R}^{3}}\widehat{g}_{n}\left(\left\|\mathbf{p}\right\|,k\right)e^{i\mathbf{p}\cdot\mathbf{r}}d\mathbf{p}=\frac{1}{2\pi^{2}r}\sum_{j=0}^{n-1}\left(2k^{2}\right)^{j}\int_{0}^{\infty}\frac{p\sin\left(pr\right)}{\left(p^{2}+k^{2}\right)^{j+1}}dp, \tag{4.3}$$

where the last integral is available in [13, Formula 3.737.2] leading to (4.1). □

Remark 3. We want to estimate the significant support of g_n, $g_{n}\left(r,k\right)\geq\varepsilon$ as a function of k. Ignoring constant factors, we observe from (4.1) that the term in (4.1) $e^{-kr}r^{n-2}k^{n-1}$ decays slower than other terms. To estimate its significant support, we consider $e^{-kr}r^{n-2}k^{n-1}\geq\varepsilon$, so that

$$r\leq k^{-1}\log_{10}\left(\varepsilon^{-1}\right)+k^{-1}\left(n-2\right)\log_{10}r+k^{-1}\left(n-1\right)\log_{10}k. \tag{4.4}$$

Although r appears on both sides of this inequality, the factor $\log_{10}r$ is negative for $r\leq1$ and, since we are interested in distances $\mathcal{O}\left(k^{-1}\log_{10}k\right)$, the second term in (4.4) can be dropped. For a given ε, as k becomes

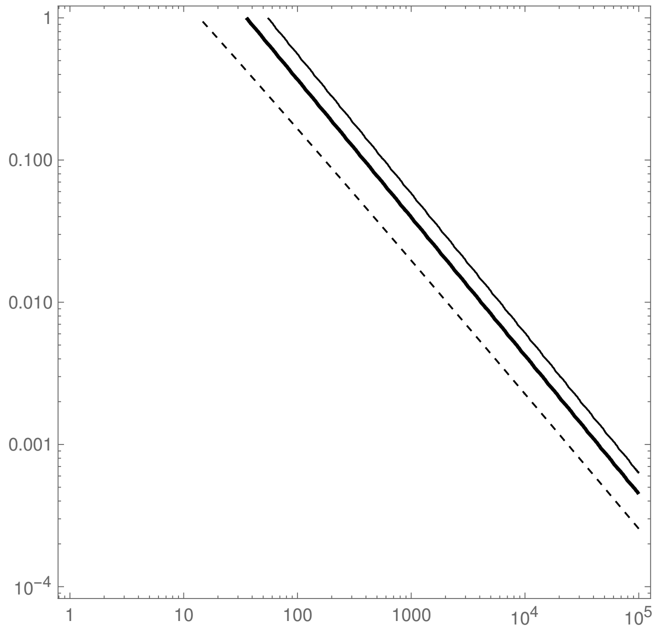

FIGURE 4.1. Log-log contour plot of the non-oscillatory component $g_8(r(k),k)$ in (4.1) for different values of ε and $1 \leq k \leq 10^5$, where thin line corresponds to $\varepsilon = 10^{-16}$, thick line to $\varepsilon = 10^{-9}$ and dashed line to 10^{-2}.

large, $g_n(r,k)$ is greater than ε within a ball of radius of $\mathscr{O}\left(c_1 k^{-1} + c_2 k^{-1} \log_{10} k\right)$. We illustrate this relation in Figure 4.1 observing that, for a fixed ε, $\log r$ is essentially proportional to $-\log k$.

Next we consider the difference between the real part of G in (1.1) and g_n,

$$q_n(r,k) = \mathscr{R}e\left(g_{n,oscill}\right)(r,k) = \frac{1}{4\pi}\frac{\cos kr}{r} - g_n(r,k), \tag{4.5}$$

and examine its behavior at $r = 0$.

Lemma 4. *The difference*

$$\mathscr{R}e\left(g_{n,oscill}\right)(\mathbf{r},k) = \frac{1}{4\pi}\frac{\cos k\|\mathbf{r}\|}{\|\mathbf{r}\|} - g_n(\|\mathbf{r}\|,k), \tag{4.6}$$

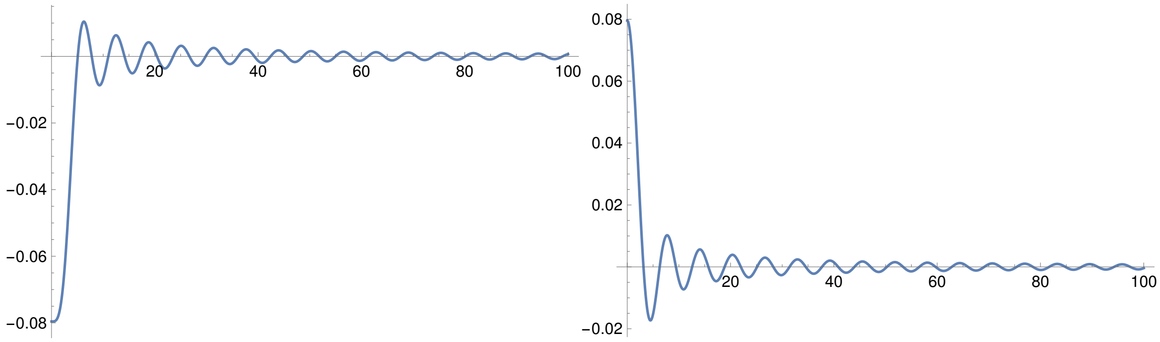

(a) (b)

FIGURE 4.2. The real part $\mathscr{Re}\left(g_{4,oscill}\right)(r,k)=\frac{1}{4\pi}\cos(kr)/r-g_4(r,k)$ (4.5) (a) and the imaginary part $\frac{1}{4\pi}\sin(kr)/r$ of the oscillatory component (b) for $k=1$.

has continuous partial derivatives at zero up to order $2n-2$. The Taylor expansion of q_n at $r=\|\mathbf{r}\|=0$ yields

$$
\begin{aligned}
q_1(r,k) &= \frac{k}{4\pi}\left(1-kr+\mathscr{O}\left((kr)^2\right)\right)\\
q_2(r,k) &= \frac{k}{4\pi}\left(-\frac{(kr)^2}{3}+\frac{(kr)^3}{6}+\mathscr{O}\left((kr)^4\right)\right)\\
q_3(r,k) &= \frac{k}{4\pi}\left(-\frac{1}{2}-\frac{(kr)^2}{12}+\frac{7(kr)^4}{240}-\frac{(kr)^5}{90}+\mathscr{O}\left((kr)^6\right)\right)\\
q_4(r,k) &= \frac{k}{4\pi}\left(-1+\frac{(kr)^4}{120}-\frac{(kr)^6}{840}+\frac{(kr)^7}{2520}+\mathscr{O}\left((kr)^8\right)\right)\\
q_5(r,k) &= \frac{k}{4\pi}\Big(-\frac{13}{8}+\frac{(kr)^2}{16}+\frac{(kr)^4}{320}-\frac{(kr)^6}{40320}+\\
&\quad \frac{83(kr)^8}{2903040}-\frac{(kr)^9}{113400}+\mathscr{O}\left((kr)^{10}\right)\Big)\\
&\cdots\ .
\end{aligned}
\tag{4.7}
$$

Proof. The function q_n in (4.5) is the inverse Fourier transform of rotationally invariant function (3.4),

$$
\mathscr{Re}\left(g_{n,oscill}\right)(r,k)=\frac{1}{2\pi^2 r}\text{p.v.}\int_0^\infty \frac{p}{p^2-k^2}\frac{\left(2k^2\right)^n}{\left(p^2+k^2\right)^n}\sin(pr)\,dp. \tag{4.8}
$$

Formally $\mathscr{Re}\left(g_{n,oscill}\right)$ in (4.8) is an even function of r and, as long as the necessary derivatives exist, only even powers can appear in its Taylor expansion. Taking $2n-2$ derivatives of $g_{n,oscill}(r,k)$ with respect to r correspond to multiplying the integrand in (4.8) by powers p^j, $0<j\leq 2n-2$ which changes the rate of decay of the integrand from $\mathscr{O}\left(p^{-2n-1}\right)$ to as low as $\mathscr{O}\left(p^3\right)$ so that the integrals for these derivatives exist. Replacing r by $\|\mathbf{r}\|$, we observe that continuous partial derivatives at zero exist up to the order $2n-2$. As we see in (4.7), the next term in the expansion does not yield a continuous derivative of (4.6) at zero. Several examples of expansions of (4.5) using (4.1) are presented in (4.7) . □

In Figure 4.2 we plot $g_{4,oscill}$ to illustrate the behavior of this oscillatory component.

5. SPATIAL REPRESENTATIONS IN $\mathbb{R}^2$

To avoid confusion, we denote the inverse Fourier transform of (3.5) in dimension $d=2$ as $h_n(r)$. We have

Lemma 5. *The inverse Fourier transform of (3.5) in dimension $d=2$ yields*

$$h_n(r,k) = \frac{1}{2\pi}\sum_{j=0}^{n-1}\frac{(kr)^j}{j!}K_j(kr), \tag{5.1}$$

where K is the modified Bessel function of the second kind.

Proof. Using (3.5), we obtain

$$\begin{aligned} h_n(r,k) &= \frac{1}{(2\pi)^2}\int_{\mathbb{R}^2}\widehat{g}_n(\|\mathbf{p}\|)\,e^{i\mathbf{p}\cdot\mathbf{r}}d\mathbf{p} \\ &= \frac{1}{2\pi}\sum_{j=0}^{n-1}\int_0^\infty \frac{\left(2k^2\right)^j}{\left(p^2+k^2\right)^{j+1}}J_0(pr)\,p\,dp \end{aligned} \tag{5.2}$$

The integral in (5.2) is available in [13, Formula 6.565.4] leading to (5.1).

Next we consider the difference between the real part of G in (1.1) and h_n in dimension $d=2$,

$$v_n(r,k) = \mathscr{R}e\left(h_{n,oscill}\right)(r,k) = -\frac{1}{4}Y_0(kr) - h_n(r,k), \tag{5.3}$$

and examine its behavior at $r=0$. □

Lemma 6. *The difference*

$$\mathscr{R}e\left(h_{n,oscill}\right)(\mathbf{r},k) = -\frac{1}{4}Y_0(k\|\mathbf{r}\|) - h_n(\|\mathbf{r}\|,k) \tag{5.4}$$

has continuous partial derivatives at $\|\mathbf{r}\|=0$ up to order $2n$. The Taylor expansion of $v_n(r,k)$ yields

$$\begin{aligned} v_1(r,k) &= \frac{-1+\gamma-\log 2}{4\pi}(kr)^2 + \mathscr{O}\left((kr)^2\log(kr)\right) \\ v_2(r,k) &= -\frac{1}{2\pi} - \frac{1}{8\pi}(kr)^2 + \frac{5-4\gamma+4\log 2}{128\pi}(kr)^4 + \mathscr{O}\left((kr)^4\log(kr)\right) \\ v_3(r,k) &= -\frac{1}{\pi} + \frac{1}{64\pi}(kr)^4 + \frac{-4+3\gamma-3\log 2}{1728\pi}(kr)^6 + \mathscr{O}\left((kr)^6\log(kr)\right) \\ v_4(r,k) &= -\frac{5}{3\pi} + \frac{1}{12\pi}(kr)^2 + \frac{1}{192\pi}(kr)^4 - \frac{5}{6912\pi}(kr)^6 \\ &+ \frac{11-8\gamma+8\log 2}{147456\pi}(kr)^8 + \mathscr{O}\left((kr)^8\log(kr)\right) \\ v_5(r,k) &= -\frac{8}{3\pi} + \frac{1}{6\pi}(kr)^2 - \frac{1}{3456\pi}(kr)^6 + \frac{1}{55296\pi}(kr)^8 \\ &+ \frac{-169+120\gamma-120\log 2}{110592000\pi}(kr)^{10} + \mathscr{O}\left((kr)^{10}\log(kr)\right) \\ &\cdots, \end{aligned} \tag{5.5}$$

where γ is Euler's constant.

Proof. The function v_n in (5.3) is the inverse Fourier transform of rotationally invariant function (3.4) in dimension $d=2$,

$$\mathscr{R}e\left(h_{n,oscill}\right)(r,k) = \frac{1}{2\pi}\int_0^\infty \frac{p}{p^2-k^2}\frac{\left(2k^2\right)^n}{\left(p^2+k^2\right)^n}J_0(pr)\,p\,dp.$$

We use the same argument to count the number of continuous derivatives of $h_{n,oscill}(\mathbf{r},k)$ as in Lemma 4. Several examples of expansions of (5.3) using (5.1) are presented in (5.5) . □

6. Integral representations

Integral representations via Gaussians of kernels of non-oscillatory operators have been used as a starting point to obtain their accurate multiresolution approximations via a linear combination of Gaussians, see e.g. [18, 8, 4, 9, 10, 5, 17, 1]. For any $\varepsilon > 0$, kernels are approximated with accuracy ε by a linear combination of Gaussians where the number of terms is shown to be $\mathscr{O}\left(\left(\log\varepsilon^{-1}\right)^2 + \log\delta^{-1}\right)$, where δ defines the interval of validity of the approximation, e.g. $\delta < r < \delta^{-1}$ (see e.g. [10]). This estimate is somewhat conservative since the actual number of terms appears to be $\mathscr{O}\left(\log\varepsilon^{-1} + \log\delta^{-1}\right)$. In what follows we construct integral representations via Gaussians of the non-oscillatory components of the Green's function (1.1).

Lemma 7. *The function $g_n(r,k)$ in dimension $d=3$ has an integral representation*

$$g_n(r,k) = \int_{-\infty}^{\infty} e^{-r^2e^t/4} w_n(k,t)\,dt \tag{6.1}$$

where

$$w_n(k,t) = \frac{1}{8\pi^{3/2}} e^{-k^2e^{-t}+\frac{1}{2}t} \left(\sum_{j=0}^{n-1} \frac{\left(2k^2e^{-t}\right)^j}{j!}\right).$$

Proof. Using the integral (see e.g. [10, eq. 2])

$$\rho^{-j-1} = \frac{1}{j!}\int_{-\infty}^{\infty} e^{-\rho e^t+(j+1)t}dt,$$

we obtain from (4.3) and (3.5)

$$\begin{aligned}
g_n(r,k) &= \frac{1}{(2\pi)^3}\sum_{j=0}^{n-1}\int_{\mathbb{R}^3} \frac{\left(2k^2\right)^j}{\left(\|\mathbf{p}\|^2+k^2\right)^{j+1}} e^{i\mathbf{p}\cdot\mathbf{r}}d\mathbf{p} \\
& \quad \frac{1}{(2\pi)^3}\int_{\mathbb{R}^3}\left(\sum_{j=0}^{n-1}\frac{\left(2k^2\right)^j}{j!}\int_{-\infty}^{\infty} e^{-\left(k^2+\|\mathbf{p}\|^2\right)e^t+(j+1)t}dt\right)e^{i\mathbf{p}\cdot\mathbf{r}}d\mathbf{p} \\
&= \frac{1}{(2\pi)^3}\int_{\mathbb{R}^3}\left(\int_{-\infty}^{\infty} e^{-e^t\|\mathbf{p}\|^2}\left(\sum_{j=0}^{n-1}\frac{\left(2k^2e^t\right)^j}{j!}\right)e^{-k^2e^t+t}dt\right)e^{i\mathbf{p}\cdot\mathbf{r}}d\mathbf{p} \\
&= \int_{-\infty}^{\infty}\left(\frac{1}{(2\pi)^3}\int_{\mathbb{R}^3} e^{-e^{-t}\|\mathbf{p}\|^2}e^{i\mathbf{p}\cdot\mathbf{r}}d\mathbf{p}\right)\sum_{j=0}^{n-1}\frac{\left(2k^2e^{-t}\right)^j}{j!}e^{-k^2e^{-t}-t}dt,
\end{aligned} \tag{6.2}$$

where in the last integral we changed the order of integration and replaced t by $-t$ for convenience. Computing the inverse Fourier transform of rotationally invariant function $e^{-e^{-t}\|\mathbf{p}\|^2}$ in dimension $d=3$, we have

$$\begin{aligned}
\frac{1}{(2\pi)^3}\int_{\mathbb{R}^3} e^{-e^{-t}\|\mathbf{p}\|^2}e^{i\mathbf{r}\cdot\mathbf{p}}d\mathbf{p} &= \frac{1}{2\pi^2 r}\int_0^{\infty} e^{-e^{-t}p^2}\sin(pr)\,p\,dp \\
&= \frac{1}{8\pi^{3/2}}e^{-r^2e^t/4}e^{\frac{3}{2}t}.
\end{aligned} \tag{6.3}$$

Substituting (6.3) into (6.2), we arrive at (6.1). □

Turning to dimension $d=2$, we have

Lemma 8. *The function h_n in dimension $d=2$ has an integral representation*

$$h_n(r,k) = \int_{-\infty}^{\infty} e^{-r^2e^t/4}\omega_n(k,t)\,dt, \tag{6.4}$$

where

$$\omega_n(k,t) = \frac{1}{4\pi}e^{-k^2e^{-t}}\left(\sum_{j=0}^{n-1}\frac{\left(2k^2e^{-t}\right)^j}{j!}\right).$$

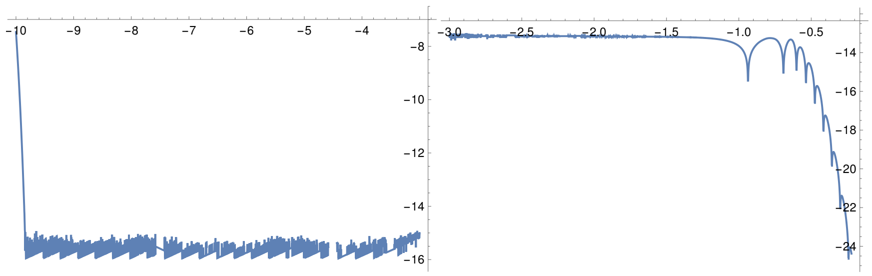

FIGURE 7.1. The relative error $e_0(10^x)$ in (7.2) for $-10 \le x \le 3$ and the absolute error $e_1(10^x)$ in (7.3) for $-3 \le x \le \log_{10}(0.44)$.

Proof. Using integral representation of functions K_j derived in [10, eq. 36], we have

$$(kr)^j K_j(kr) = 2^{j-1} k^{2j} \int_0^\infty e^{-r^2 s/4 - k^2/s} s^{-j-1} ds,$$

and, therefore,

$$\frac{1}{2\pi} \sum_{j=0}^{n-1} \frac{(kr)^j}{j!} K_j(kr) = \frac{1}{4\pi} \int_0^\infty e^{-r^2 s/4 - k^2/s} \sum_{j=0}^{n-1} \frac{(2k^2)^j}{j!} s^{-j-1} ds.$$

Changing variables $s = e^t$, we obtain (6.4). □

7. DISCRETIZATION OF INTEGRAL REPRESENTATIONS

Spatial integral representations of non-oscillatory components in (6.1) and (6.4) lead to approximations of functions g_n and h_n by a linear combination of Gaussians. In both cases, for $r > \delta$, the integrands decay super exponentially for $t \to \pm\infty$, where the rate of decay for $t \to -\infty$ is controlled by k. Heuristically, by selecting a finite interval of integration so that the integrands and their derivatives are negligible outside that interval, any user selected accuracy ε can be achieved using the trapezoidal rule. The resulting sum is a linear combination of Gaussians which may be viewed as a multiresolution approximation of the non-oscillatory component.

As a result, we obtain a separated multiresolution approximation of the kernel of the non-oscillatory component of the Helmholtz operator. There are several approaches to apply this kernel rapidly in $\mathcal{O}\left(k^d \left(\log \varepsilon^{-1}\right)^2\right)$ operations, for example via algorithms in [3] or via the Fast Gauss transform in [15, 16]. We refer to [7, 6] for the details of algorithms for applying both the oscillatory and the non-oscillatory (singular) components.

As an example, we describe an approximation of $g_4(r,k)$ where $k = 100$. We discretize the integral in (6.1) as

$$\widetilde{g}_4(r,k) = \Delta \sum_{m=20}^{200} e^{-r^2 e^{m\Delta}/4} w_4(k, m\Delta), \quad \Delta = \frac{1}{4}, \quad k = 100, \quad r = \|\mathbf{r}\|. \tag{7.1}$$

Near the singularity of $g_4(r,k)$, on the interval $10^{-10} \le r \le 10^{-3}$, we use the relative error

$$e_0(r) = \log_{10} \left| \frac{g_4(r,k) - \widetilde{g}_4(r,k)}{g_4(r,k)} \right|, \tag{7.2}$$

and on the interval $10^{-3} \le r \le 40/k + 2\log_{10} k/k$ (or $10^{-3} \le r \le 44/100$, see Remark 3) the absolute error,

$$e_1(r) = \log_{10} \left| g_4(r,k) - \widetilde{g}_4(r,k) \right|. \tag{7.3}$$

These approximation errors are illustrated in Figure 7.1. The terms of the linear combination of Gaussians in (7.1) can be applied to a function in parallel. Also we note that the Gaussians with large exponents can be treated as approximations to a delta function and such terms can be combined reducing the overall number of terms.

8. On motivation and further work

The derivation of explicit expressions for splitting the Helmholtz Green's function into a sum of oscillatory and non-oscillatory (singular) components was motivated, in part, by an application of such splitting to solving boundary-value problems (BVPs), specifically to the evaluation of layer potentials close to the boundary for Laplace and Helmholtz problems. What is described below has not been implemented and is presented as a motivation for further development.

Solving boundary-value problems (BVPs) for Laplace and Helmholtz equations using boundary integral equations (BIEs) reduces the dimension of the problem and leads to well behaved integral equations on the boundary. Once the BIE is solved and the density function on the boundary is obtained, an integral over the boundary involving a Green's function (e.g. double-layer potential) provides a formula to evaluate the solution at any target point in the domain. However, in the vicinity of the boundary, the straightforward evaluation of this integral is expensive. We refer to [2], which mentions several approaches to speedup the evaluation and considers the so-called quadrature by expansion (QBX) method. The key observation of QBX is that the solution can be evaluated via its expansion in a neighborhood of any point near the boundary while using the kernel only at a sufficient distance away from the boundary.

From a general point of view, the question is how to efficiently evaluate kernels with singularities. For volumetric integrals arising in non-oscillatory problems, a multiresolution approximation of kernels and potentials with singularities via a linear combination of Gaussians yields efficient algorithms. This approach is widely used in non-relativistic and relativistic quantum chemistry (QC), see e.g. [18, 17, 11, 1] and references therein. The recent paper [19] applies the approximation of kernels via Gaussians within a new version of the Fast Multipole Method. It is a natural approach since both, kernels and their approximations, are rotationally invariant.

For non-oscillatory boundary values problems, approximations of Green's functions via a linear combination of Gaussians can also be used for the evaluation of layer potentials close to the boundary. Given a density function on the boundary computed via a BIE, the solution of the BVP can be efficiently evaluated at any target point in the domain, including points arbitrarily close to the boundary. Approaching the singularity of the kernel at the boundary, the domain of integration shrinks due to the rapid growth of exponents of the Gaussian terms. As a result, the cost of evaluation of the integral remains at (worst) constant for each term of the Gaussian expansion; in fact, the necessary number of terms is small since those with large exponents are evaluated explicitly. Several special cases of such an approach are described in [10] for the Laplace's equation.

For oscillatory boundary values problems, explicit formulas splitting the kernel into two components provide an efficient way for evaluating layer potentials in the immediate vicinity of the boundary. Specifically, since the oscillatory component can have any finite number of continuous derivatives (see Lemma 4 and Lemma 6), the boundary integral for this component may be evaluated at any point via a quadrature used for solving the BIE. Only the non-oscillatory component has a singularity but, being represented via Gaussians, it can be applied in a multiresolution fashion as in the case of non-oscillatory problems (see Section 7).

Recall that, away from the boundary, the non-oscillatory component is negligible (indeed, the original kernel does not have a singularity in such case). Therefore, one could use either the oscillatory component or the original kernel. An interesting question is whether there is any advantage in using the oscillatory component rather than the original kernel.

We plan to implement the approach described above, compare it with existing methods and report results separately.

9. Conclusions

The Helmholtz operator appears in many problems of mathematical physics and is also part of more complicated Green's functions. In particular, the components of the Dyadic Green's function in electromagnetics are derivatives of the Helmholtz Green's function. Therefore, the splitting into the oscillatory and the non-oscillatory components can be obtained for the Dyadic Green's function as well. We expect several problems beyond the one described in this paper to be addressed using our results.

10. Acknowledgments

The author would like to thank Brad Alpert (NIST) and Lucas Monzón (CU) for suggestions to improve the manuscript.

References

[1] J. Anderson, R.J. Harrison, B. Sundahl, W. S. Thornton, and G. Beylkin. Real-space quasi-relativistic quantum chemistry. *Computational and Theoretical Chemistry*, 1175:112711, 2020.

[2] A. H. Barnett. Evaluation of layer potentials close to the boundary for Laplace and Helmholtz problems on analytic planar domains. *SIAM Journal on Scientific Computing*, 36(2):A427–A451, 2014.

[3] G. Beylkin, V. Cheruvu, and F. Pérez. Fast adaptive algorithms in the non-standard form for multidimensional problems. *Appl. Comput. Harmon. Anal.*, 24(3):354–377, 2008.

[4] G. Beylkin, R. Cramer, G.I. Fann, and R.J. Harrison. Multiresolution separated representations of singular and weakly singular operators. *Appl. Comput. Harmon. Anal.*, 23(2):235–253, 2007.

[5] G. Beylkin, G. Fann, R. J. Harrison, C. Kurcz, and L. Monzón. Multiresolution representation of operators with boundary conditions on simple domains. *Appl. Comput. Harmon. Anal.*, 33:109–139, 2012. http://dx.doi.org/10.1016/j.acha.2011.10.001.

[6] G. Beylkin, C. Kurcz, and L. Monzón. Fast algorithms for Helmholtz Green's functions. *Proc. R. Soc. A*, 464(2100):3301–3326, 2008. doi:10.1098/rspa.2008.0161.

[7] G. Beylkin, C. Kurcz, and L. Monzón. Fast convolution with the free space Helmholtz Green's function. *J. Comp. Phys.*, 228(8):2770–2791, 2009.

[8] G. Beylkin and M. J. Mohlenkamp. Algorithms for numerical analysis in high dimensions. *SIAM J. Sci. Comput.*, 26(6):2133–2159, July 2005.

[9] G. Beylkin, M. J. Mohlenkamp, and F. Pérez. Approximating a wavefunction as an unconstrained sum of Slater determinants. *Journal of Mathematical Physics*, 49(3):032107, 2008.

[10] G. Beylkin and L. Monzón. Approximation of functions by exponential sums revisited. *Appl. Comput. Harmon. Anal.*, 28(2):131–149, 2010.

[11] G. Beylkin, L. Monzón, and X. Yang. Adaptive algorithm for electronic structure calculations using reduction of Gaussian mixtures. *Proceedings of the Royal Society A*, 475(2226):20180901, 2019.

[12] I. M. Gel'fand and G. E. Shilov. *Generalized functions. Vol. 1*. Academic Press, New York, 1964. Properties and operations, Translated from the Russian by Eugene Saletan.

[13] I. S. Gradshteyn, I. M. Ryzhik, A. Jeffrey, and D. Zwillinger. *Table of integrals, series, and products*. Academic Press, 7 edition, 2007.

[14] L. Grafakos. *Classical and modern Fourier analysis*. Pearson Education, Inc., 2004.

[15] L. Greengard and J. Strain. The fast Gauss transform. *SIAM J. Sci. Stat. Comput.*, 12(1):79–94, 1991.

[16] L. Greengard and X. Sun. A new version of the fast Gauss transform. In *Proceedings of the international congress of mathematicians*, volume III (Extra Vol.), pages 575–584, 1998.

[17] R. J. Harrison, G. Beylkin, F. A. Bischoff, J. A. Calvin, G. I. Fann, J. Fosso-Tande, D. Galindo, J.R Hammond, R. Hartman-Baker, J.C. Hill, J. Jia, J.S. S. Kottmann, M-J. Y. Ou, L.E. Ratcliff, M.G. Reuter, A.C. Richie-Halford, N.A. Romero, H. Sekino, W.A. Shelton, B.E. Sundahl, W.S. Thornton, E.F. Valeev, A. Vázquez-Mayagoitia, N. Vence, and Y. Yokoi. MADNESS: a Multiresolution, ADaptive Numerical Environment for Scientific Simulation. *SIAM J. Sci. Comput.*, 38(5):S123–S142, 2016.

[18] R.J. Harrison, G.I. Fann, T. Yanai, Z. Gan, and G. Beylkin. Multiresolution quantum chemistry: basic theory and initial applications. *J. Chem. Phys.*, 121(23):11587–11598, 2004.

[19] S. Jiang and L. Greengard. A Dual-space Multilevel Kernel-splitting Framework for Discrete and Continuous Convolution. 2023. https://arxiv.org/abs/2308.00292.

Department of Applied Mathematics, University of Colorado at Boulder, UCB 526, Boulder, CO 80309-0526